Inorganic Chemistry

Article

pubs.acs.org/IC

Near-IR Electrochromic Film Prepared by Oxidative Electropolymerization of the Cyclometalated Pt(II) Chloride with a Triphenylamine Group

Dongfang Qiu,* Xiaoyu Bao, Qian Zhao, Qichao Yang, Yuquan Feng, Hongwei Wang, Chunxia Yang, and Kecheng Liu

College of Chemistry and Pharmacy Engineering, Nanyang Normal University, Nanyang 473061, People's Republic of China

Supporting Information

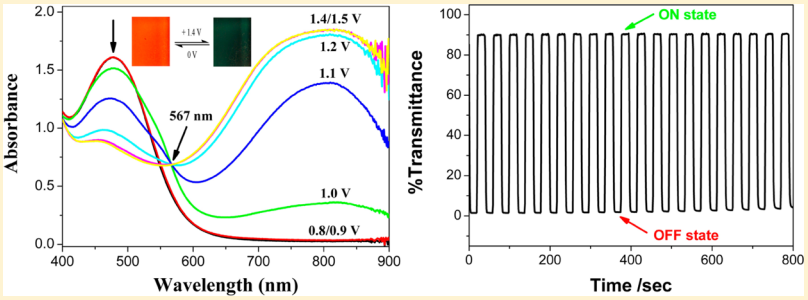

ABSTRACT: A cyclometalated platinum chloride [(**L**)PtCl] {**L** = 4-[*p*-(diphenylamino)phenyl]-6-phenyl-2,2′-bipyridine} was successfully synthesized and characterized by ^{1}H NMR, ^{13}C NMR, MALDI-TOF MS, elemental analysis, and X-ray crystallography. Its oxidative electropolymerization proceeds smoothly on the working Pt and ITO electrodes by cyclic voltammetry. The film thickness can be easily tuned by controlling the CV scan number. The orange hybrid polymer film shows the nondiffusion-controlled redox processes and a unusually inverse dependence of ac impedance on its thickness. As a result of switching of the MLCT/ICT and dication absorption transitions, the adherent metallopolymer film exhibits the low-voltage-controlled anodic coloration near-IR electrochromism with significant optical contrast ratio (ΔT% = 88.8% at 820 nm), fast response time (1.9 s for the coloration step and 2.3 s for the bleaching step), and high coloration efficiency (*CE* = 363.3 $C^{-1}\cdot cm^2$).

INTRODUCTION

Near-IR electrochromic (NIR-EC) materials with high optical contrast and coloration efficiency (*CE*), long-term stability, fast response time, and low switching potential are strongly desirable for practical uses in the military or civilian area.[1] The most widely studied NIR-EC candidates are organic conducting polymers such as polyaniline (PANI),[2] poly(3,4-ethylenedioxythiophene) (PEDOT), and their derivatives,[3] in which dibenzyl poly(3,4-propylenedioxythiophene) (PProDOT-Bz_2)[3c] and poly(hexyl-3,4-ethylenedioxyselenophene) (PEDOS-C_6)[3e] have the highest known optical contrast ratio (ΔT%) of 88−89%.

Metallopolymers, generated from metal−polypyridine complexes via metal-ion-induced self-assembly[4] and electrochemical techniques,[5] are a promising class of electrochromic materials, because of their multichromophoric properties and multiredox nature with color changes in the regular potential window. However, most of them display the anodic decoloration effect in the visible region associated with the M(III)/M(II) interconversion. Yao recently reported the NIR electrochromism of oxidative or reductive electropolymerization (EP) films of cyclometalated bisruthenium complexes, which is attributed to the intervalence charge-transfer (IVCT) transition.[6]

Our group reported the electrochromic effects of metallopolymers generated by oxidative EP of [(C^N^N)PtCl] complexes with the *N*-alkyl-diphenylamine (ΔT% = 70.5% at 667 nm, 5.8 s for the coloration step, and *CE* = 441.4 $C^{-1}\cdot cm^2$)[7] and carbazole-grafted *N*-alkyl-diphenylamine substituent groups (ΔT% = 67.3% at 615 nm, 3.1 s for the coloration step, and *CE* = 132 $C^{-1}\cdot cm^2$),[8] which show the anodic colaration in the visible region with high optical contrast ratios, comparable response times, and black coloration efficiencies. In order to further extend their spectral response to the NIR region and enhance their electrochromic performance, a triphenylamine (TPA) unit, which is expected to simultaneously serve as an electropolymerizable site and a good charge transfer moiety, was incorporated at the 4 position of the cyclometalated Pt(II) chloride. Its structure and EP behavior and the spectroelectrochemical and dynamic electrochromic characterization of the electrodeposited film in solution were mainly investigated.

Received: April 8, 2015
Published: August 13, 2015

DOI: 10.1021/acs.inorgchem.5b00782
Inorg. Chem. 2015, 54, 8264−8270

EXPERIMENTAL SECTION

Materials and General Procedures. The commercially available regents 2-acetylpyridine, 4-bromobenzaldehyde, ammonium formate, diphenylamine, anhydrous K_2CO_3, CuI, 18-crown-6, and K_2PtCl_4 were analytical grade and used as received without further purification. Reactions under argon atmosphere were carried out in oven-dried glassware using standard Schlenk techniques. Tin(IV)-doped indium oxide (ITO) was purchased from Shenzhen Nanbo Display Technology Co. Ltd. (10 Ω/□) and cleaned by sonicating 15 min in 1:1:5 $NH_4OH-H_2O_2-H_2O$ and rinsing with water and ethanol before using. Tetrabutylammonium perchlorate ($^nBu_4NClO_4$) was prepared[7] and used as the supporting electrolyte for electrochemical studies.

Caution! *Perchlorate salts are potentially explosive and should be handled with care and in small amounts.*

Synthesis of 4-[*p*-(Diphenylamino)phenyl]-6-phenyl-2,2′-bipyridine (HL). A mixture of diphenylamine (2.55 g, 15.0 mmol), 4-(*p*-bromophenyl)-6-phenyl-2,2′-bipyridine (3.87 g, 10.0 mmol), anhydrous K_2CO_3 (4.15 g, 30 mmol), CuI (0.19 g, 1.0 mmol), and 18-crown-6 (0.13 g, 0.5 mmol) was heated to 185 °C under an argon atmosphere for 12 h. After the reaction mixture was cooled to room temperature, $CHCl_3$ and H_2O were added in turn. The organic phase was washed with distilled H_2O, dried over anhydrous sodium sulfate, and then concentrated. The residue was purified by column chromatography (Al_2O_3, petroleum ether/CH_2Cl_2 = 2:1 (v/v)). Ligand HL was obtained as a white needle crystal by recrystallizing from its MeOH/ethyl acetate solution in a yield of 63%. ^{1}H NMR (400 MHz, $CDCl_3$): δ 8.73 (d, *J* = 4.8 Hz, 1H), 8.70 (d, *J* = 8.0 Hz, 1H), 8.65 (s, 1H), 8.22 (d, *J* = 7.2 Hz, 2H), 7.98 (s, 1H), 7.88 (t, *J* = 7.6 Hz, 1H), 7.73 (d, *J* = 8.4 Hz, 2H), 7.54 (t, *J* = 7.4 Hz, 2H), 7.47 (t, *J* = 7.2 Hz, 1H), 7.37−7.29 (m, 5H), 7.19 (t, *J* = 8.4 Hz, 6H), 7.10 (t, *J* = 7.4 Hz, 2H). ^{13}C NMR (100 MHz, $CDCl_3$): δ 157.1, 156.4, 156.1, 149.6, 149.0, 148.8, 147.4, 139.6, 136.9, 131.9, 129.4, 129.0, 128.7, 128.0, 127.1, 124.8, 123.7, 123.4, 123.1, 121.5, 117.8, 116.9. Matrix-assisted laser desorption/ionization time-of-flight mass spectrometry (MALDI-TOF MS): *m*/*z* = 475.2 ([M], $C_{34}H_{25}N_3$ requires 475.2). Anal. Calcd: C, 85.87; H, 5.30; N, 8.84. Found: C, 85.68; H, 5.24; N, 8.75.

Synthesis of [(L)PtCl]. A mixture of HL (0.48 g, 1.0 mmol), K_2PtCl_4 (0.42 g, 1.0 mmol), and glacial acetic acid (50 mL) was refluxed overnight under an argon atmosphere in the absence of light. After cooling to room temperature, the reaction mixture was filtered, and the crude solid was recrystallized from its MeOH/CH_2Cl_2 solution three times to form the desired product as a red crystal in a yield of 58%. ^{1}H NMR (400 MHz, DMSO-d_6): δ 8.89 (d, *J* = 5.2 Hz, 1H), 8.69 (d, *J* = 8.4 Hz, 1H), 8.44 (s, 1H), 8.35 (t, *J* = 8.0 Hz, 1H), 8.18 (s, 1H), 8.01 (d, *J* = 8.8 Hz, 2H), 7.90 (t, *J* = 7.0 Hz, 1H), 7.77 (d, *J* = 8.0 Hz, 1H), 7.48 (d, *J* = 7.2 Hz, 1H), 7.39 (t, *J* = 8.0 Hz, 4H), 7.18−7.12 (m, 7H), 7.09−7.04 (m, 3H). ^{13}C NMR (100 MHz, $CDCl_3$): δ 165.9, 157.2, 154.1, 150.2, 149.9, 148.5, 146.9, 146.6, 142.3, 138.8, 135.1, 130.7, 129.7, 129.6, 128.0, 126.9, 125.3, 124.1, 123.9, 123.8, 122.6, 122.2, 115.6, 115.1. MALDI-TOF MS: *m*/*z* = 705.1 ([M] + 1, $C_{34}H_{24}ClN_3Pt$ requires 704.1). Anal. Calcd: C, 57.92; H, 3.43; N, 5.96. Found: C, 57.71; H, 3.35; N, 5.78.

Instrumentation. NMR spectra were recorded on Bruker AV 400 spectrometers and referenced with respect to tetramethylsilane, $Si(CH_3)_4$, internal standard. MALDI-TOF MS analyses were performed by using a Bruker Autoflex III mass spectrometer. Elemental analyses were carried out on a Bio-Rad Co's elemental analytical instrument. The surface morphology and energy-dispersive X-ray spectroscopy (EDS) of the polymer film were determined on a FEI-Quanta 200 scanning electron microscope (SEM) with a XL30ESEM-FEG. IR spectra were recorded by using a powder sample pelletized with KBr on a Nicolet 170 SXFT-IR spectrophotometer over the range 4000−225 cm^{-1}. UV−vis absorption spectra were obtained on a PerkinElmer Lambda 650s UV−vis spectrophotometer. PL spectra were performed on a PerkinElmer LS50B spectrometer. Cyclic voltammetry (CV) was conducted on a CHI660A electrochemical workstation. The ac impedance spectra were measured in the frequency range from 1 to 100 kHz at +0.50 V vs saturated calomel electrode (SCE) in 0.1 mol·dm^{-3} Bu_4NClO_4/CH_2Cl_2 solution with the presence of 1.0 × 10^{-3} mol·dm^{-3} ferrocene as a redox probe.

X-ray Crystallography. A suitable single crystal of [(L)PtCl] (0.24 mm × 0.21 mm × 0.18 mm) was used for structure determination. Crystal diffraction data of [(L)PtCl] were collected on a Bruker SMART APEX-II CCD diffractometer equipped with graphite-monochromated Mo Kα radiation (λ = 0.71073 Å) at 296(2) K using the Φ−ω scan mode. In the range of 2.22° < *q* < 25.00° with −20 ≤ *h* ≤ 18, −10 ≤ *k* ≤ 9, and −22 ≤ *l* ≤ 20, a total of 12 827 reflections were collected, among which 4778 were unique (R_{int} = 0.0526). Absorption correction was applied by using the SADABS.[9] The structure was solved by direct methods and refined by full-matrix least-squares techniques on F^2 with the SHELX-97 package.[10] All non-hydrogen atoms were refined anisotropically and hydrogen atoms isotropically by full-matrix least-squares refinement. The organic hydrogen atoms were generated geometrically.

RESULTS AND DISCUSSION

Synthesis and Characterization. The syntheses of HL and [(L)PtCl] explored in this work are shown in Scheme S1 (Supporting Information (SI)). 4-[*p*-(Diphenylamino)phenyl]-6-phenyl-2,2′-bipyridine (HL) was synthesized by Ullmann condensation between diphenylamine and 4-(*p*-bromophenyl)-6-phenyl-2,2′-bipyridine, followed by chromatographic purification. The cyclometalated Pt(II) chloride [(L)PtCl] was synthesized by refluxing HL and K_2PtCl_4 in glacial acetic acid. After recrystallization from its MeOH/CH_2Cl_2 solution three times, red crystals of the desired product were obtained in medium yield. Both of them have good solubility in CH_2Cl_2 and were characterized by ^{1}H NMR, COSY ^{1}H/^{1}H NMR (SI, Figures S1 and S2), ^{13}C NMR, MALDI-TOF MS, and elemental analysis.

Crystal Structure. The single crystals of complex [(L)PtCl] (CCDC: 991879) was grown by slowly evaporating the solvent from its concentrated CH_2Cl_2/MeOH solution. The crystal data and crystal structure parameters are listed in Table 1, and the perspective view is shown in Figure 1. The coordination geometry of the Pt atom shows a distorted square planar configuration with C(16)−Pt(1)−N(1) and N(2)−Pt(1)−Cl(1) angles of 161.1(3)° and 179.8(2)°. The bond distances of Pt−C(16), Pt−N(1), and Pt−N(2) are 2.078(7), 2.041(7), and 1.948(7) Å, respectively, which are comparable to those of previously reported analogues.[11] The C(16)−C(11)−C(10)−N(2) and N(2)−C(6)−C(5)−N(1) torsion angles of 0.4(10)° and −1.1(9)° suggest that the configuration of the (C^N^N) ligand is basically planar. The phenyl ring at the 4 position is efficiently conjugated to the [(C^N^N)Pt] moiety, as evidenced by the C(7)−C(8)−C(17)−C(22) and C(9)−C(8)−C(17)−C(18) torsion angles of 12.7(13)° and 13.3(12)°. The geometry of the N(3) atom is a distorted tetrahedral configuration with the C(20)−N(3)−C(23), C(20)−N(3)−C(29), and C(23)−N(3)−C(29) angles of 120.6(7)°, 121.8(7)°, and 117.6(7)°, respectively. As shown in Figure 2, the crystal lattice of [(L)PtCl] is packed by one kind of alternately arranged dimeric units, which are parallel to each other along the *b* axis. The two [(L)PtCl] molecules in each unit are stacked in a head-to-tail fashion with an interplanar separation of 3.334 Å, suggesting the π−π interaction between their (C^N^N) ligands. The Pt−Pt distance of 6.255 Å indicates that the metal−metal stacking interaction is absent.

Photophysical Properties. The UV−vis absorption spectrum of [(L)PtCl] in CH_2Cl_2 solution exhibits intense

DOI: 10.1021/acs.inorgchem.5b00782
Inorg. Chem. 2015, 54, 8264−8270

Table 1. Crystal Data and Crystal Structure Parameters

compound	[(L)PtCl]
empirical formula	$C_{34}H_{24}ClN_3Pt$
fw	705.10
temp. (K)	296(2)
wavelength (Å)	0.71073
cryst syst	monoclinic
space group	$P2(1)/c$
a (Å)	16.933(3)
b (Å)	8.7398(14)
c (Å)	18.576(3)
α (deg)	90.00
β (deg)	98.852(3)
γ (deg)	90.00
vol. (Å^3)	2716.4(8)
Z	4
D_{calcd} (g·cm^{-3})	1.724
abs coeff (mm^{-1})	5.293
$F(000)$	1376
cryst size (mm)	0.24 × 0.21 × 0.18
θ range for data collection (deg)	2.22 to 25.00
limiting indices	$-20 \le h \le 18, -10 \le k \le 9, -22 \le l \le 20$
completeness to θ = 25.00°	99.7%
data/restraints/params	4778/18/352
goodness-of-fit on F^2	1.075
final R indices [$I > 2\sigma(I)$][a]	R_1 = 0.0510, wR_2 = 0.1495
R indices (all data)	R_1 = 0.0627, wR_2 = 0.1579
largest diff. peak and hole (e·Å^{-3})	2.324 and −2.656

[a] $R_1 = \sum||F_o| - |F_c||/\sum|F_o|$, $wR_2 = \{\sum w[(F_o)^2 - (F_c)^2]^2/\sum w[(F_o)^2]^2\}^{1/2}$.

bands at 250−350 nm and less intense bands at 350−550 nm (Figure S3). With reference to previous spectroscopic work on 6-phenyl-2,2′-bipyridyl (C^N^N) platinum(II) chlorides,[12] the high-energy intense absorption bands are clearly assigned to the singlet $\pi \rightarrow \pi^*$ intraligand (IL) transitions of the (C^N^N) ligand. Noticeably, compared with that of complex [(4-phenyl-C^N^N)PtCl] (λ_{max} = 434 nm, ε = 4.80 × 10^3 dm^3·mol^{-1}·cm^{-1}),[13] the low-energy absorption band of [(L)PtCl] (λ_{max} = 452 nm, ε = 18.7 × 10^3 dm^3·mol^{-1}·cm^{-1}) is apparently red shifted and have a 3−4 times increase in intensity after introduction of the TPA group. This observation is consistent with previous work, where introduction of the electron-donating TPA group at the 4′ position of 2,2′:6′,2″-terpyridine (TPY),[14] alkoxyl substituent on 4,6-diphenyl-2,2′-bipyridine ligand,[15] and *N*-alkyl-substituted arylamino or bis-arylamino units at the para position of 4-phenyl-C^N^N[13] also led to similar effects. Such behavior is strongly indicative of the π(TPA) → π^*(C^N^N) intraligand charge transfer (ICT) transition involved in the low-energy band, overlapping with the well-known spin-allowed singlet dπ(Pt) → π^*(C^N^N) metal-to-ligand charge transfer (MLCT) transition. Excited at 450 nm, [(L)PtCl] shows a strong emission at λ_{max} = 590 nm.

The electrochemical behavior of HL and [(L)PtCl] was also investigated by CV in CH_2Cl_2 solutions. Because the oxidation potential of the (C^N^N) ligand is beyond the potential window of the solvent, the single anodic peak at $E_{p,a}$ = +1.10 V (vs saturated calomel electrode (SCE)) in the cyclic voltammogram of HL accords to losing a single electron from the TPA unit to form a radical cation species.[16] The cyclic voltammo-

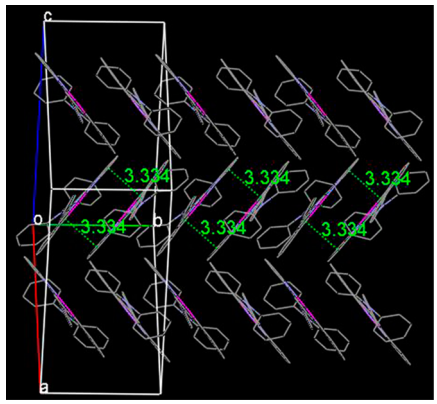

Figure 2. Crystal packing of complex [(L)PtCl] (hydrogen atoms have been omitted for clarity).

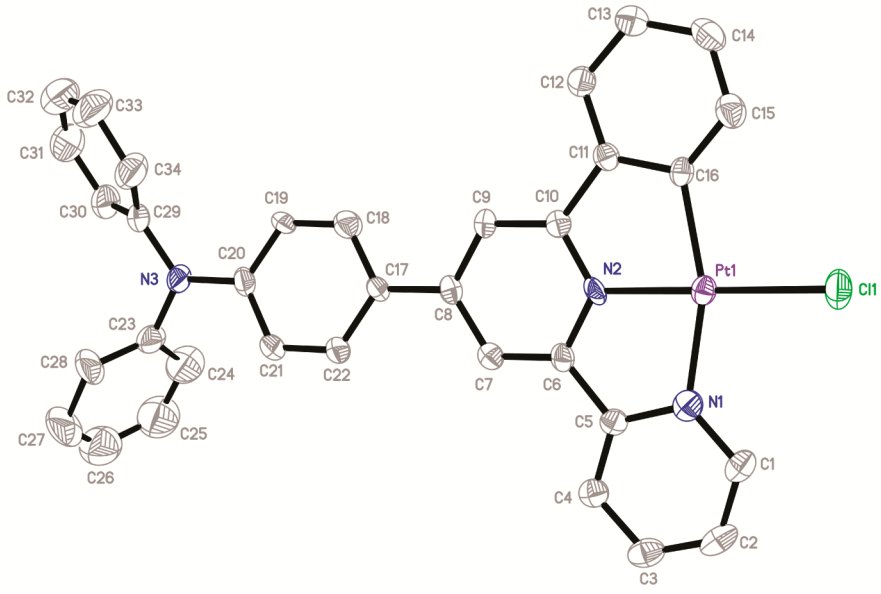

Figure 1. Perspective view of the single-crystal structure of [(L)PtCl] with 30% thermal ellipsoids (hydrogen atoms have been omitted for clarity).

DOI: 10.1021/acs.inorgchem.5b00782
Inorg. Chem. 2015, 54, 8264−8270

gram of [(L)PtCl] shows two irreversible redox waves at $E_{p,a}$ = +0.93 and +1.08 V (vs SCE), which can be reasonably assigned to the Pt(III/II)-based and TPA-based oxidation processes.

Electrochemical Polymerization (EP). The CV technique was used for the EP of [(L)PtCl] in a 0.1 M Bu_4NClO_4/CH_2Cl_2 solution containing 0.5 mM monomer. The repetitive cyclic voltammograms are shown in Figure 3, in which the

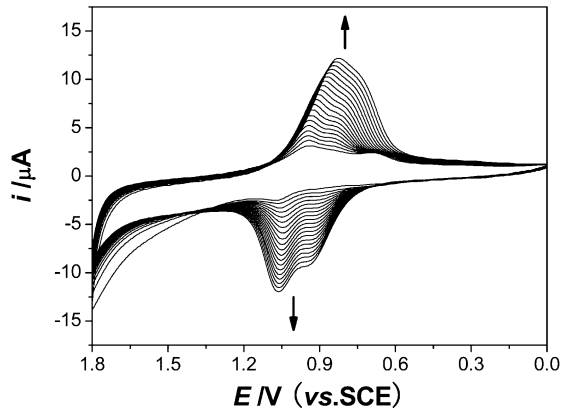

Figure 3. Cyclic voltammograms of [(L)PtCl] on a Pt disk electrode at 50 mV·s^{-1}.

metal-based and TPA-based redox waves gradually increase, indicating the formation of a conductive polymer. Upon washing with CH_2Cl_2 and ethanol to remove the unreacted monomer and oligomeric species, a compact orange film is present on the working Pt disk electrode surface, and it shows poorly resolved redox waves in monomer-free electrolytic solution, especially at fast potential scan rates (Figure 4). Both

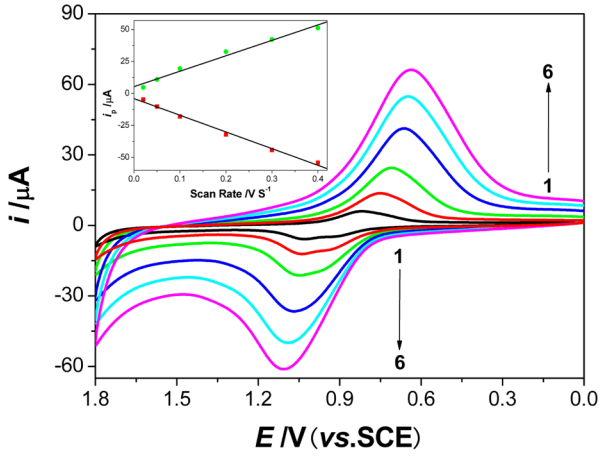

Figure 4. Cyclic voltammograms of the poly-[(L)PtCl] film on a Pt electrode at different scan rates of 25 (1), 50 (2), 100 (3), 200 (4), 300 (5), and 400 (6) mV·s^{-1}. (Inset) Linear dependence of the peak currents as a function of scan rate.

anodic and cathodic currents are linearly dependent on the potential scan rates (Figure 4, inset), indicating the non-diffusion-controlled redox processes in the well-adhered polymer film.

Poly-[(L)PtCl] film-coated Pt electrodes with different coverages were obtained from the parallel solutions with a constant monomer concentration by controlling the CV scan number. Figure 5 shows the ac impedance spectra of poly-[(L)PtCl] film-coated Pt electrodes after 10, 20, 30, and 40 CV

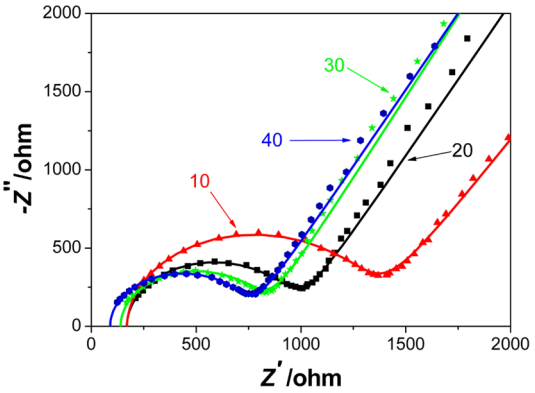

Figure 5. Impedance spectra ($-Z''$ vs Z') of the poly-[(L)PtCl] film-coated Pt disk electrodes obtained after 10, 20, 30, and 40 CV scan cycles in the EP process.

scan cycles. The equivalent circuit is shown in Figure 6, whose typical elements for each electrode are summarized in Table 2.

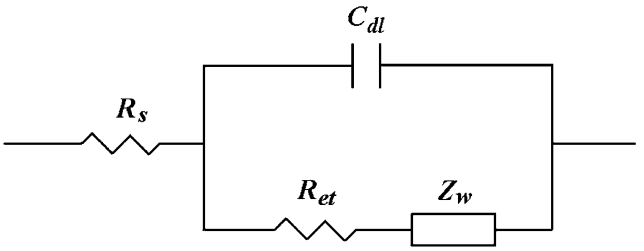

Figure 6. Equivalent circuit proposed for the poly-[(L)PtCl] film-coated Pt electrodes.

Table 2. Solution Resistance (R_s), Electron Transfer Resistance (R_{et}), and Capacity (C_{dl}) of Poly-[(L)PtCl]/ITO Electrodes Obtained after 10, 20, 30, and 40 CV Scan Cycles in the EP Process

electrode name	R_s (Ω)	R_{et} (Ω)	C_{dl} (F/cm^2)
poly-[(L)PtCl]-10	170	1160	8.0×10^{-8}
poly-[(L)PtCl]-20	170	800	8.0×10^{-8}
poly-[(L)PtCl]-30	130	670	8.0×10^{-8}
poly-[(L)PtCl]-40	90	660	8.0×10^{-8}

As shown in Figure 5, each ac impedance spectrum is fitted by a semicircle at high frequencies, and the diameter of the fitted semicircle decreases with increasing the CV scan number in the EP process. Because the diameter of the semicircle corresponds to the electron transfer resistance (R_{et}), the result suggests that the more CV scan number used in the EP process, the easier charge transfer from the electrolyte to the Pt electrode surface. Our previous studies proved that the *N*-alkyl-substituted diphenylamine (DPA) functionalized bis-TPY Ru(II)[17] and Fe(II)[18] complexes can be oxidatively electropolymerized to form the metallopolymers composed of alternating [M-$(TPY)_2$]$^{2+}$ and bis-DPA segments. Also, the ac impedances of these metallopolymers increased with the CV scan number in their EP processes. However, in this paper, poly-[(L)PtCl] film shows an inverse dependence of ac impedance on its thickness. This similar effect was also observed in our previously reported [(C^N^N)PtCl]-based metallopolymer films,[7,8] likely suggesting a different formation mechanism of the planar four-

DOI: 10.1021/acs.inorgchem.5b00782
Inorg. Chem. 2015, 54, 8264−8270

coordinate d^8 Pt(II) chloride and the presence of highly conductive units in it.

Spectroelectrochemical and Electrochromic Characterization.[7,8] In order to allow the spectroscopic studies, EP of [(**L**)PtCl] was also performed on transparent indium tin oxide (ITO) electrode. The CV behavior of [(**L**)PtCl] on an ITO electrode is similar to that on a Pt electrode, except for shifts of redox waves due to the resistance of the ITO layer (Figure 7).

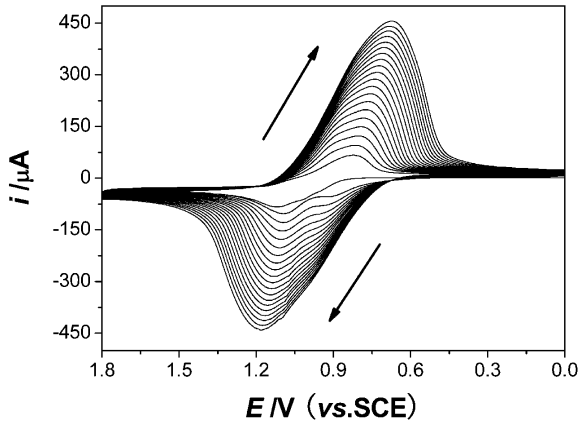

Figure 7. Oxidative EP of [(**L**)PtCl] on an ITO electrode.

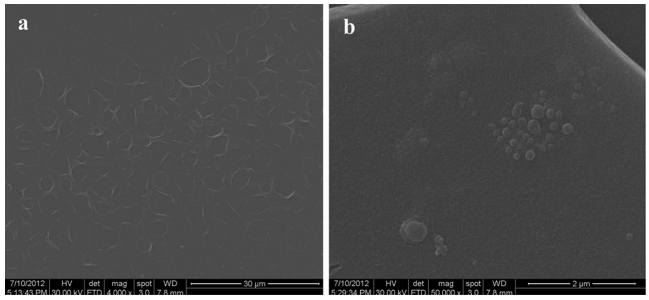

Figure 8. SEM images of poly-[(**L**)PtCl] film/ITO electrodes obtained after 5 (a) and 30 (b) CV scan cycles in EP process.

During the EP process, the discontinuous island (Figure 8a) and the island-on-layer morphologies (Figure 8b) are observed at initial and final growth stages, respectively. Using the monomer solutions with a constant concentration, the film thickness is easily modulated by controlling the CV scan number in the EP process (Figure 9).

The spectroelectrochemical property of poly-[(**L**)PtCl] film on ITO electrode was performed at various applied potentials (Figure 10). Before +0.8 V, the poly-[(**L**)PtCl] film in neutral form exhibits the red-shifted and enhanced MLCT/ICT band at λ_{max} = 478 nm. As the applied potential becomes more anodic to 1.4 V, the MLCT/ICT band is decreased gradually in intensity with the formation of a new broad band centered at around 820 nm. The new absorption band is reasonably attributed to the dication formation by full oxidation of the electro-cross-linking TPA segments in the metallopolymer film.[19] The clear isosbestic point at 567 nm suggests the conversion between the neutral and the fully oxidized states of poly-[(**L**)PtCl] film, and the intense NIR absorption band indicates that the dication form of the metallopolymer is

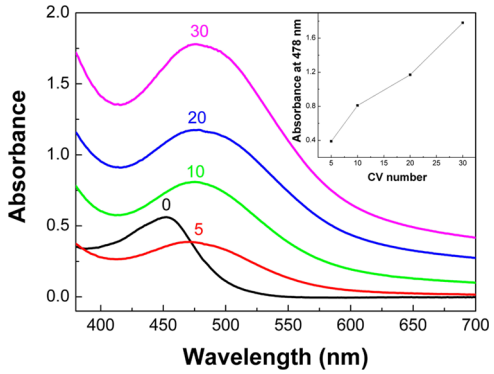

Figure 9. Absorption spectra of monomer [(**L**)PtCl] in CH_2Cl_2 solution (0) and poly-[(**L**)PtCl]/ITO electrodes obtained after 5, 10, 20, and 30 CV scan cycles in EP process. (Inset) Relationship between the absorbance of poly-[(**L**)PtCl]/ITO electrodes at 478 nm and the CV scan number.

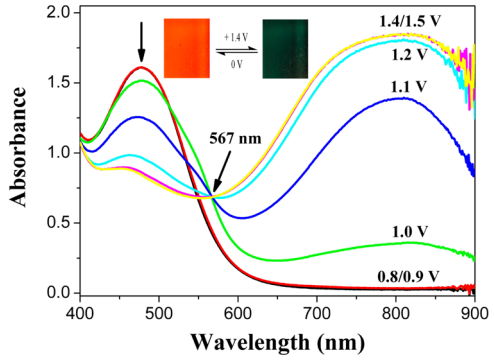

Figure 10. Spectroelectrochemical spectra of the poly-[(**L**)PtCl] film/ITO electrode upon stepwise application of potential from 0 to +1.4 V vs Ag wire reference electrode. (Inset) Color changes at different potentials.

relatively stable at room temperature.[20] The polymer film undergoes a clear color change from orange to greenish black.

The dynamic electrochromic experiment of poly-[(**L**)PtCl] film on ITO electrode was carried out at 820 nm, where the maximum transmittance difference between its neutral and its fully oxidized states was observed. The potential was step switched between 0 and +1.4 V at regular intervals of 20 s. As indicated in Figure 11, the times required for 95% full transmittance changes are 1.9 s for the coloration step and 2.3 s for the bleaching step. The optical contrast ratio (ΔT%) of 88.8% is achieved from the coloration transmittance of 1.4% (the turn-OFF state) and the bleaching transmittance of 90.2% (the turn-ON state) at the first potential switching step, which is comparable to the highest known optical contrast ratio (ΔT% = 88−89%) of PProDOT-Bz_2[3c] and PEDOS-C_6[3e] and much higher than those of our previously reported Pt(II) complexes.[7,8] After consecutive switching between 0.0 and 1.4 V over 45 cycles, the metallopolymer film still exhibits good reversibility and stability (ΔT% = 86.0%). The black coloration efficiency and bleaching efficiency are 363.3 and 380.0 $C^{-1}\cdot cm^2$, respectively.

Formation Mechanism of the Electrodeposited Film. Because the EP polymer is virtually insoluble in most organic solvents, its structural characterization by conventional NMR and mass spectroscopy cannot be achieved. However, the EDS analysis (SI, Figures S4 and S5) of poly-[(**L**)PtCl] film clearly suggests the 1:2 ratio of Pt and Cl atoms in this material, and

DOI: 10.1021/acs.inorgchem.5b00782
Inorg. Chem. 2015, 54, 8264−8270

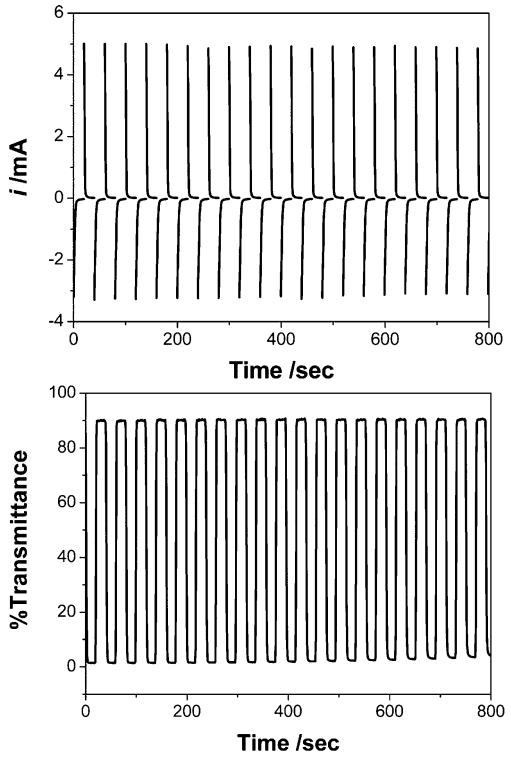

Figure 11. Dynamic changes of the current and transmittance of the poly-[(**L**)PtCl] film/ITO electrode upon switching the potential between 0 and +1.4 V with a pulse width of 20 s. Transmittance changes monitored at λ = 820 nm as a function of time.

the strong peak at ν = 1097.6 cm^{-1} in its FT-IR spectrum (SI, Figure S6) definitely proves the presence of the Cl═O functional group.[21] These results likely indicate that the ClO_4^- ions of the supporting electrolyte participate in the EP process as the counteranions. Additionally, previous studies have revealed that the square-planar Pt(II) complexes with cyclometalating ligands can aggregate through Pt···Pt and/or $\pi-\pi$ interactions to prepare the organoplatinum-based quasi-one-dimensional nanomaterials.[22] Therefore, on the basis of the evidence collected above and with the crystallographic and electrochemical experiment facts, a possible EP mechanism is given in Scheme 1, involving (1) an irreversible one-electron electrochemical oxidation of [(**L**)PtCl] followed by the electrostatic attraction of one ClO_4^- anion from the supporting electrolyte, (2) self-aggregation through the $\pi-\pi$ interactions between the (C^N^N) ligands to form the dimer (**A**) with two peripheral TPA groups, (3) upon electrochemical oxidation at higher potential, one peripheral TPA group transforms into a radical cation intermediate, which triggers the C−C bond formation on the para position of the terminal benzene to give the **A** dimer (**B**). In this process, the electron-deficient $[(C^N^N)PtCl]_2^{2+}$ core plays a key role in the stabilization of the radical cation species.[23] (4) with consecutive anodic scans, the chain propagation preferentially takes from the two terminal TPA units of **B** to give the hybrid metallopolymer composed of alternating bis(cyclometalated platinum chloride) and bis-TPA segments.[6d] Owing to the dimerization of planar π-conjugated [(C^N^N)PtCl] units, the embedding of ClO_4^- counteranions, and the presence of *N*,*N*′,*N*′-tetraphenyl-4,4′-diaminobiphenyl (TPB) segments, the polymer shows the unusually inverse dependence of ac impedance on its thickness, fast response time, and characterized NIR dication absorption band upon oxidation, as described above in the electrochemical and spectroelectrochemical studies.

CONCLUSIONS

In summary, a novel metallopolymer film has been prepared through oxidative electropolymerization of the TPA-substituted cyclometalated platinum(II) chloride. The adherent film

Scheme 1. Proposed EP Mechanism of [(L)PtCl]

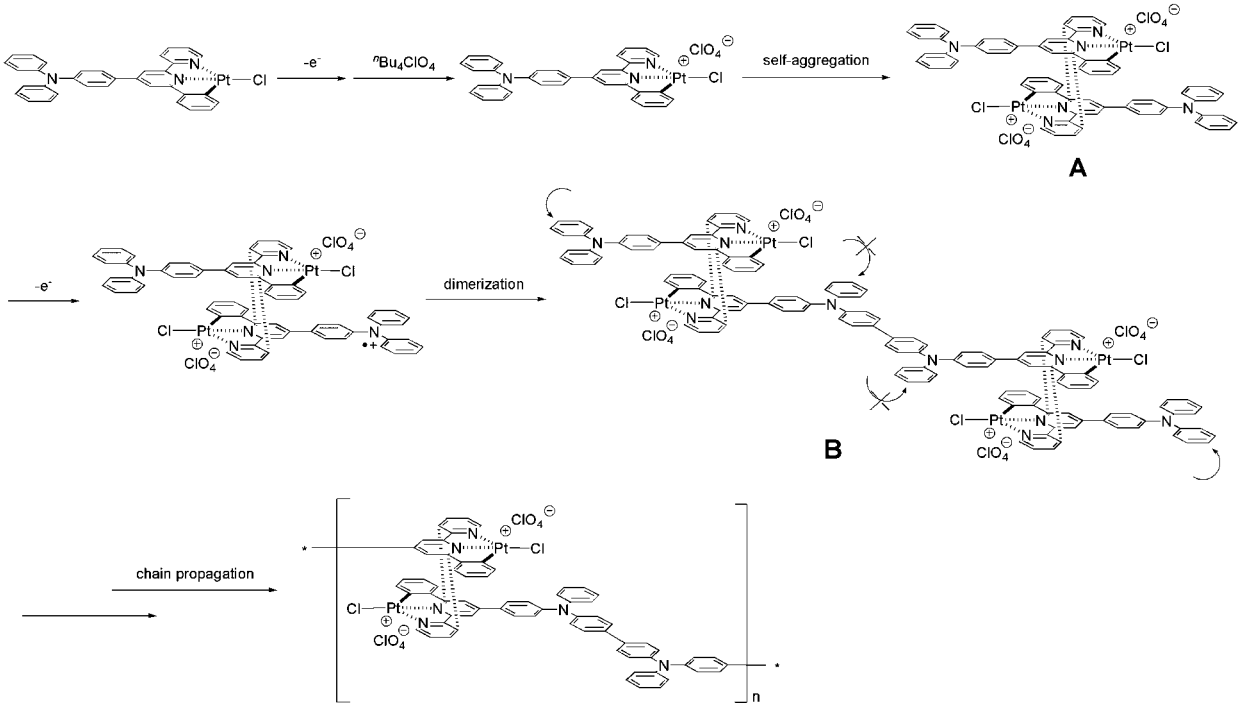

DOI: 10.1021/acs.inorgchem.5b00782
Inorg. Chem. 2015, 54, 8264−8270

exhibits the low-voltage-controlled anodic coloration NIR electrochromism with significant optical contrast ratio ($\Delta T\%$ = 88.8% at 820 nm), fast response time (1.9 s for the coloration step and 2.3 s for the bleaching step), and high coloration efficiency (CE = 363.3 $C^{-1}\cdot cm^2$) as a result of reversible switching of the MLCT/ICT and dication absorption transitions. The result indicates that this hybrid film has a potential use as an electro-optic switch in the NIR optical communication device. Studies on further expanding its spectral response range and improving its stability are currently being investigated in this laboratory.

■ ASSOCIATED CONTENT

Supporting Information

The Supporting Information is available free of charge on the ACS Publications website at DOI: 10.1021/acs.inorgchem.5b00782.

X-ray crystallographic data of [(**L**)PtCl] in CIF format; characterization of H**L** and [(**L**)PtCl]; UV−vis absorption and PL emission spectra of H**L** and [(**L**)PtCl]; EDS spectra of poly-[(**L**)PtCl] film; FT-IR spectra of [(**L**)PtCl] and poly-[(**L**)PtCl] (PDF)

■ AUTHOR INFORMATION

Corresponding Author

*E-mail: qiudf2008@163.com.

Notes

The authors declare no competing financial interest.

■ ACKNOWLEDGMENTS

We thank the Natural Science Foundation of Henan Province (102300410221), the Natural Science Foundation of Nanyang Normal University (ZX2010012), and the Young Core Instructor Project of the Education Commission of Henan Province for funding support.

■ REFERENCES

(1) (a) Fabian, J.; Nakazumi, H.; Matsuoka, M. *Chem. Rev.* **1992**, *92*, 1197. (b) Qian, G.; Wang, Z. Y. *Chem. - Asian J.* **2010**, *5*, 1006.

(2) (a) Chou, M.-Y.; Leung, M.-K.; Su, Y. O.; Chiang, C. L.; Lin, C.-C.; Liu, J.-H.; Kuo, C.-K.; Mou, C.-Y. *Chem. Mater.* **2004**, *16*, 654. (b) Lee, C.-W.; Seo, Y.-H.; Lee, S.-H. *Macromolecules* **2004**, *37*, 4070. (c) Natera, J.; Otero, L.; Sereno, L.; Fungo, F.; Wang, N.-S.; Tsai, Y.-M.; Hwu, T.-Y.; Wong, K.-T. *Macromolecules* **2007**, *40*, 4456. (d) Yen, H.-J.; Lin, K.-Y.; Liou, G.-S. *J. Mater. Chem.* **2011**, *21*, 6230. (e) Yen, H.-J.; Lin, H.-Y.; Liou, G.-S. *Chem. Mater.* **2011**, *23*, 1874. (f) De Simone, B. C.; Quartarolo, A. D.; Cospito, S.; Veltri, L.; Chidichimo, G.; Russo, N. *Theor. Chem. Acc.* **2012**, *131*, 1225.

(3) (a) Beaujuge, P. M.; Reynolds, J. R. *Chem. Rev.* **2010**, *110*, 268. (b) Amb, C. M.; Dyer, A. L.; Reynolds, J. R. *Chem. Mater.* **2011**, *23*, 397. (c) Krishnamoorthy, K.; Ambade, A. V.; Kanungo, M.; Contractor, A. Q.; Kumar, A. J. *J. Mater. Chem.* **2001**, *11*, 2909. (d) Groenendaal, L. B.; Zotti, G.; Aubert, P.-H.; Waybright, S. M.; Reynolds, J. R. *Adv. Mater.* **2003**, *15*, 855. (e) Li, M.; Patra, A.; Sheynin, Y.; Bendikov, M. *Adv. Mater.* **2009**, *21*, 1707. (f) Chandrasekhar, P.; Zay, B. J.; Birur, G. C.; Rawal, S.; Pierson, E. A.; Kauder, L.; Swanson, T. *Adv. Funct. Mater.* **2002**, *12*, 95. (g) Kim, B.; Kim, J.; Kim, E. *Macromolecules* **2011**, *44*, 8791.

(4) (a) Maier, A.; Rabindranath, A. R.; Tieke, B. *Adv. Mater.* **2009**, *21*, 959. (b) Zhang, C.-F.; Liu, A.; Chen, M.; Nakamura, C.; Miyake, J.; Qian, D.-J. *ACS Appl. Mater. Interfaces* **2009**, *1*, 1250. (c) Motiei, L.; Lahav, M.; Freeman, D.; van der Boom, M. E. *J. Am. Chem. Soc.* **2009**, *131*, 3468. (d) Welterlich, I.; Tieke, B. *Macromolecules* **2011**, *44*, 4194. (e) Kurth, D. G.; López, J. P.; Dong, W.-F. *Chem. Commun.* **2005**, 2119. (f) Tieke, B. *Curr. Opin. Colloid Interface Sci.* **2011**, *16*, 499. (g) Han, F. S.; Higuchi, M.; Kurth, D. G. *Adv. Mater.* **2007**, *19*, 3928. (h) Han, F. S.; Higuchi, M.; Kurth, D. G. *J. Am. Chem. Soc.* **2008**, *130*, 2073.

(5) (a) Milum, K. M.; Kim, Y. N.; Holliday, B. J. *Chem. Mater.* **2010**, *22*, 2414. (b) Powell, A. B.; Bielawski, C. W.; Cowley, A. H. *J. Am. Chem. Soc.* **2010**, *132*, 10184. (c) Powell, A. B.; Bielawski, C. W.; Cowley, A. H. *J. Am. Chem. Soc.* **2009**, *131*, 18232. (d) Matsuse, R.; Abe, M.; Tomiyasu, Y.; Inatomi, A.; Yonemura, H.; Yamada, S.; Hisaeda, Y. *J. Inorg. Organomet. Polym. Mater.* **2013**, *23*, 136.

(6) (a) Yao, C.-J.; Zhong, Y.-W.; Yao, J. *J. Am. Chem. Soc.* **2011**, *133*, 15697. (b) Wang, L.; Yang, W.-W.; Zheng, R.-H.; Shi, Q.; Zhong, Y.-W.; Yao, J. *Inorg. Chem.* **2011**, *50*, 7074. (c) Yao, C.-J.; Sui, L.-Z.; Xie, H.-Y.; Xiao, W.-J.; Zhong, Y.-W.; Yao, J. *Inorg. Chem.* **2010**, *49*, 8347. (d) Yao, C.-J.; Zhong, Y.-W.; Yao, J. *Inorg. Chem.* **2013**, *52*, 10000. (e) Yao, C.-J.; Zhong, Y.-W.; Nie, H.-J.; Abruña, H. D.; Yao, J. *J. Am. Chem. Soc.* **2011**, *133*, 20720.

(7) Qiu, D.; Bao, X.; Zhao, Q.; Feng, Y.; Wang, H.; Liu, K. *J. Mater. Chem. C* **2013**, *1*, 695.

(8) Qiu, D.; Bao, X.; Feng, Y.; Liu, K.; Wang, H.; Shi, H.; Guo, Y.; Huang, Q.; Zeng, J.; Zhou, J.; Xing, Z. *Electrochim. Acta* **2012**, *60*, 339.

(9) Sheldrick, G. M. *SADABS, Program of Empirical Absorption Correction for Area Detector Data*; University of Göttingen: Göttingen, Germany, 1996.

(10) Sheldrick, G. M. *SHELX-97, Program for Crystal Structure Analysis*; University of Göttingen: Göttingen, Germany, 1997.

(11) (a) Lai, S. W.; Chan, M. C. W.; Cheung, K. K.; Che, C. M. *Organometallics* **1999**, *18*, 3327. (b) Lai, S. W.; Lam, H. W.; Lu, W.; Cheung, K. K.; Che, C. M. *Organometallics* **2002**, *21*, 226. (c) Hofmann, A.; Dahlenburg, L.; van Eldik, R. *Inorg. Chem.* **2003**, *42*, 6528.

(12) Lu, W.; Mi, B. X.; Chan, M. C. W.; Hui, Z.; Che, C. M.; Zhu, N.; Lee, S. T. *J. Am. Chem. Soc.* **2004**, *126*, 4958.

(13) Qiu, D.; Wu, J.; Xie, Z.; Cheng, Y.; Wang, L. *J. Organomet. Chem.* **2009**, *694*, 737.

(14) (a) Chung, S. K.; Tseng, Y. R.; Chen, C. Y.; Sun, S. S. *Inorg. Chem.* **2011**, *50*, 2711. (b) Mahato, P.; Saha, S.; Das, A. *J. Phys. Chem. C* **2012**, *116*, 17448. (c) Goodall, W.; Williams, J. A. G. *Chem. Commun.* **2001**, 2514.

(15) Shao, P.; Li, Y.; Azenkeng, A.; Hoffmann, M. R.; Sun, W. *Inorg. Chem.* **2009**, *48*, 2407.

(16) Qiu, D.; Cheng, Y.; Wang, L. *Dalton Trans.* **2009**, 3247.

(17) Qiu, D.; Zhao, Q.; Bao, X.; Liu, K.; Wang, H.; Guo, Y.; Zhang, L.; Zeng, J.; Wang, H. *Inorg. Chem. Commun.* **2011**, *14*, 296.

(18) Bao, X.; Qiu, D.; Wang, H.; Liu, K.; Guo, Y.; Niu, Z. *Chin. Mater. Rev.* **2012**, *26*, 81.

(19) (a) Huang, W. S.; MacDiarmid, A. G. *Polymer* **1993**, *34*, 1833. (b) Fu, Y.; Weiss, R. A. *Synth. Met.* **1997**, *84*, 103. (c) Shimano, J. Y.; MacDiarmid, A. G. *Synth. Met.* **2001**, *123*, 251. (d) Cai, J.; Ma, L.; Niu, H.; Zhao, P.; Lian, Y.; Wang, W. *Electrochim. Acta* **2013**, *112*, 59. (e) Cai, J.; Niu, H.; Zhao, P.; Ji, Y.; Ma, L.; Wang, C.; Bai, X.; Wang, W. *Dyes Pigm.* **2013**, *99*, 1124. (f) Yen, H.-J.; Chen, C.-J.; Liou, G.-S. *Adv. Funct. Mater.* **2013**, *23*, 5307. (g) Ma, L.; Niu, H.; Cai, J.; Lian, Y.; Zhang, C.; Wang, C.; Bai, X.; Wang, W. *Sens. Actuators, B* **2013**, *188*, 117. (h) Yen, H.-J.; Liou, G.-S. *J. Mater. Chem.* **2010**, *20*, 9886.

(20) (a) Sadighi, J. P.; Singer, R. A.; Buchwald, S. L. *J. Am. Chem. Soc.* **1998**, *120*, 4960. (b) Goodson, F. E.; Hauck, S. I.; Hartwig, J. F. *J. Am. Chem. Soc.* **1999**, *121*, 7527. (c) Zhang, X.-X.; Sadighi, J. P.; Mackewitz, T. W.; Buchwald, S. L. *J. Am. Chem. Soc.* **2000**, *122*, 7606. (d) Chen, R.; Benicewicz, B. C. *Macromolecules* **2003**, *36*, 6333.

(21) Koo, C.-K.; Ho, Y.-M.; Chow, C.-F.; Lam, M. H.-W.; Lau, T.-C.; Wong, W.-Y. *Inorg. Chem.* **2007**, *46*, 3603.

(22) Lu, W.; Roy, V. A. L.; Che, C.-M. *Chem. Commun.* **2006**, 3972.

(23) Leung, M.; Chou, M. Y.; Su, Y. O.; Chiang, C. L.; Chen, H. L.; Yang, C. F.; Yang, C. C.; Lin, C. C.; Chen, H. T. *Org. Lett.* **2003**, *5*, 839.

DOI: 10.1021/acs.inorgchem.5b00782
Inorg. Chem. 2015, 54, 8264−8270